Available online at www.sciencedirect.com
SCIENCE DIRECT
Journal of Molecular Catalysis A: Chemical 245 (2006) 272–277
JOURNAL OF MOLECULAR CATALYSIS A: CHEMICAL
www.elsevier.com/locate/molcata

Comparative study on oxidation of methane to ethane and ethylene over Na_2WO_4–Mn/SiO_2 catalysts prepared by different methods

Jiaxin Wang, Lingjun Chou, Bing Zhang, Huanling Song, Jun Zhao, Jian Yang, Shuben Li *

State Key Laboratory for Oxo Synthesis and Selective Oxidation, Lanzhou Institute of Chemical Physics, Chinese Academy of Sciences and Graduate School of Chinese Academy of Sciences, Lanzhou 730000, PR China

Received 29 July 2005; received in revised form 3 August 2005; accepted 26 September 2005
Available online 10 November 2005

Abstract

The 5 wt% Na_2WO_4–2 wt% Mn/SiO_2 catalysts have been prepared by the incipient wetness impregnation method, mixture slurry method and sol–gel method, and their catalytic performances for the oxidative coupling of methane (OCM) are evaluated in a continuous micro-reactor. 30% of CH_4 conversion and 70% of C_2 selectivity have been obtained in methane-oxygen co-feed without any dilutes over these catalysts. X-ray diffraction (XRD) studies indicate that the main crystallite phases of catalysts are Mn_2O_3, Na_2WO_4 and α-cristobalite, and different precursors of silica are transformed ultimately into highly crystallite α-cristobalite. XPS results show that Na, W and Mn are mainly distributed on the surface of catalyst prepared by the incipient wetness impregnation method, but more uniform between the surface and bulk on the catalysts prepared by other two methods. Comparing with the catalyst prepared by the incipient wetness impregnation method, that of prepared by the mixture slurry method has an excellent stability and can alleviate the loss of active components during a 500 h run. Structure changes indicate that α-cristobalite is not indispensable for effective Na_2WO_4–Mn/SiO_2 catalysts.

Keywords: Na_2WO_4–Mn/SiO_2 catalyst; Oxidative coupling of methane; Prepared method

1. Introduction

The Na_2WO_4–Mn/SiO_2 catalyst, firstly reported by Li and his co-workers [1–3], has been known to be one of the most effective catalysts for the oxidative coupling of methane (OCM). In a single-pass operation, 66.9% C_2 selectivity at 37.7% CH_4 conversion with 2.6 C_2H_4/C_2H_6 ratio was obtained [1]. 81% C_2 selectivity at 20% CH_4 conversion and 80% C_2 selectivity at 33% CH_4 conversion over this catalyst had been reproduced by Lunsford [4] and Lambert [5], respectively. At an elevated pressure, the catalyst exhibited not only the same catalytic activity and C_2 selectivity, but also a higher ratio of C_2H_4 to C_2H_6 when the space velocity was increased [6]. More recently, CeO_2 and SnO_2 promoted Na–W–Mn/SiO_2 catalysts for the oxidative conversion of methane have been studied in a micro-stainless-steel reactor under elevated pressure [7–9]. A CH_4 conversion of 47.2% with a C_2–C_4 selectivity of 47.3% (C_2:C_3:C_4 = 1:1:3.3) was obtained at 710 °C with 1.0×10^5 ml g^{-1} h^{-1} GHSV, CH_4/O_2 = 2.5, and P = 0.6 MPa.

The reaction mechanism of OCM is very complicated and considerable controversies concerning the nature of the active centre in the catalyst exist. In the case of Na–W–Mn/SiO_2 catalyst Li [10] proposed a two metal active site model for OCM reaction. In this model it was believed that the active oxygen species was surface lattice oxygen O_s^{2-}, and the redox mechanism involving two metal sites, $W^{6+/5+}$ and $Mn^{3+/2+}$, could be used to explain CH_4 and O_2 activation. CH_4 was activated by O_s^{2-} to generate $CH_3^{\bullet}$ radical on $W^{6+/5+}$ site, and the electron transferred from $W^{6+/5+}$ site to $Mn^{3+/2+}$ site, which was responsible for molecular oxygen activation to form surface lattice oxygen O_s^{2-} as an active oxygen species for CH_4 activation. By comparison with catalytic behaviours of Na_2WO_4–Mn/SiO_2, Na_2WO_4–Mn/MgO, and $NaMnO_4$/MgO catalysts, Lunsford and co-workers [4,11] suggested that Na–O–Mn species were the most probable active sites, in which Mn was an active component, Na provides selectivity, and W was required to stabilize the catalyst. Lambert and co-workers [5,12] emphasized that the phase transition from amorphous silica to α-cristobalite was a

* Corresponding author.
E-mail address: lisb@lzb.ac.cn (S. Li).

1381-1169/$ – see front matter © 2005 Elsevier B.V. All rights reserved.
doi:10.1016/j.molcata.2005.09.038

crucially important requirement for the production of effective catalyst, and they proposed that Na played a dual role as both structural and chemical promoter. Recently, Ji et al. [13,14] proposed that both Na–O–Mn and Na–O–W acted as the active centres of Na_2WO_4–Mn/SiO_2 catalysts, in which there was a synergic effect of sodium, tungsten, and manganese components, and the WO_4 tetrahedron on the catalyst surface appeared to play an essential role in achieving high CH_4 conversion and high C_2 hydrocarbon selectivity in the OCM reaction.

Nevertheless, in the previous studies, Na_2WO_4–Mn/SiO_2 catalyst was usually prepared by the incipient wetness impregnation method, which made the active components were enriched on the catalyst surface and tend to loss during extended times on stream. In this paper, the effect of Na_2WO_4–Mn/SiO_2 catalysts prepared by different methods for OCM reaction was studied in detail. The essential aims were to explore appropriate method to prepare active and stable Na_2WO_4–Mn/SiO_2 catalyst, and on the other hand, to further complement the understanding of Na_2WO_4–Mn/SiO_2 catalyst from the point of preparation methods.

2. Experimental

2.1. Catalyst preparation

The 5 wt% Na_2WO_4–2 wt% Mn/SiO_2 catalysts for OCM reaction were prepared by the incipient wetness impregnation method, mixture slurry method and sol–gel method, and the three catalysts were denoted by W–Mn/SiO_2 (A), W–Mn/SiO_2 (B) and W–Mn/SiO_2 (C), respectively. All chemicals involved during preparation of catalysts included: silica particles (Qindao Ocean Chemical Plant, China), $Mn(NO_3)_2$ (50% $Mn(NO_3)_2$, A.R., Beijing Chemical Plant, China), $Na_2WO_4{\cdot}2H_2O$ (A.R., Beijing Jinghua Chemical Plant, China), and $(C_2H_5)_4SiO_4$ (A.R., Shanghai Chemical Plant, China).

2.1.1. W–Mn/SiO_2 (A): the incipient wetness impregnation method

The silica particles (40–60 mesh) were impregnated with the aqueous solutions of $Mn(NO_3)_2$ and $Na_2WO_4{\cdot}2H_2O$ in appropriate concentration at 80 °C, respectively. The impregnated silica particles were evaporated to dryness, and then dried overnight at 100 °C. Finally, the resultant was calcined in air for 8 h at 850 °C.

2.1.2. W–Mn/SiO_2 (B): the mixture slurry method

The aqueous solutions of $Mn(NO_3)_2$ and $Na_2WO_4{\cdot}2H_2O$ in appropriate concentration were added dropwise into a stirred silica sol at room temperature, respectively. The resultant were mixed well in the rotatory evaporator at 80 °C for 5 h to be homogeneous. The mixture slurry was then dried overnight at 100 °C, followed by calcined in air for 8 h at 850 °C. The catalyst sample was crushed and sieved to a size of 40–60 mesh.

2.1.3. W–Mn/SiO_2 (C): the sol–gel method

The $Mn(NO_3)_2$ and $Na_2WO_4{\cdot}2H_2O$ were added to a vessel containing a certain amount $(C_2H_5)_4SiO_4$ at a desired ratio, which was stirred vigorously for 30 min before the addition of appropriate amounts of ethanol and HNO_3, and with vigorously stirring to complete the gelation at 60 °C. The dryness and calcination of the gel were in the same way of other two methods above. After calcination, the catalyst sample was then crushed and sieved to a size of 40–60 mesh.

2.2. Catalyst characterization

X-ray diffraction patterns of fresh catalysts were obtained with a Panalytical X'pert Pro. diffractometer using Cu Kα radiation at room temperature. Diffractograms were recorded from $2\theta = 10$–80° with the detector moving in $\Delta 2\theta = 0.017^\circ$ steps to achieve good angular resolution. The specific surface areas of the catalysts were measured by BET method on an ASAP 2010 apparatus at liquid nitrogen temperature with N_2 as the absorbate.

XPS analyses of the catalysts were performed on a VG ESCALAB 210 spectrometer. The fresh catalyst was placed on sample holder pressed into a self-supported wafer. A Mg target was used as the anode of the X-ray source with a power of 200 W. The pass energy of the analyzer was 30 eV in a step increment of 0.05 eV. The binding energies were calibrated using the Si(2p) line at 103.4 eV as the reference. Near-surface compositions were calculated from peak areas using the sensitivity factors, which were provided in the software of the instrument.

Temperature-programmed desorption of oxygen (O_2-TPD) was carried out on an AMI-100 catalytic microreactor, and the products were detected with an on-line Dycor system 1000 quadrupole mass spectrometer. The heating rate was 30 °C/min and the temperature range was from room temperature to 1000 °C. Before performing an O_2-TPD experiment, the sample (0.1g) was pretreated in a helium stream at 950 °C for 20 min to remove adsorbates, followed by cooling to room temperature in O_2 and then purging with helium for 20 min. The quantification of O_2 desorbed from the catalysts was calibrated by the peak areas against a standard pulse of O_2.

2.3. Catalytic activity test

Activity testing was carried out in a quartz fixed-bed microreactor (i.d. 8 mm) at ambient atmospheric pressure. 0.2 g catalyst (40–60 mesh) was loaded in the reactor and the length of the catalyst bed was approximately 10 mm. Quartz chips was filled in the remaining space of reactor so as to reduce the contribution from gas-phase reactions. The reactants, CH_4 (99.9%) and O_2 (99.9%) without any diluents, were co-fed into the reactor. At the reactor outlet a cold trap was used to remove water from the exit gas stream. Blank runs with quartz chips showed negligible conversion at the reaction conditions. The reaction products were then analyzed with an on-line gas chromatograph equipped with a TCD, using a Poropak Q column for the separation of CH_4, CO_2, C_2H_4, and C_2H_6, and a 5A molecular sieve column for the separation of O_2, CH_4, and CO.

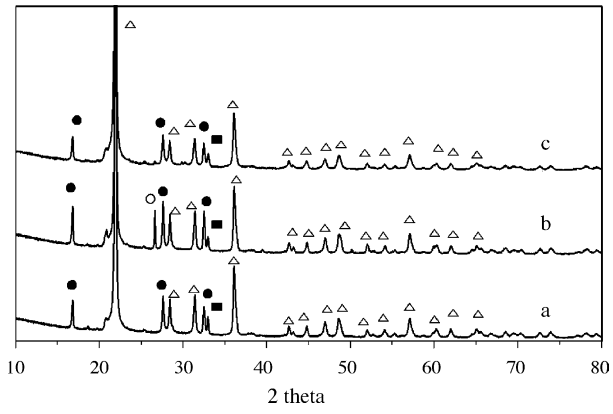

Fig. 1. The XRD pattern of (a) W–Mn/SiO_2 (A), (b) W–Mn/SiO_2 (B), and (C) W–Mn/SiO_2 (C). (●) Na_2WO_4, (■) Mn_2O_3, (△) α-cristobalite, (◯) quartz.

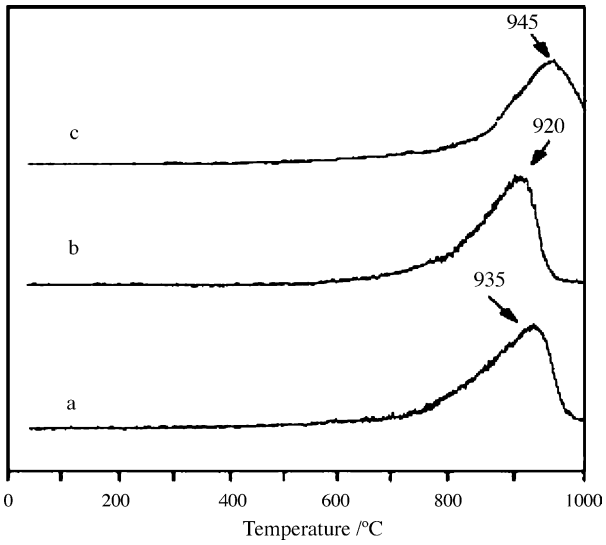

Fig. 2. O_2-TPD profiles of (a) W–Mn/SiO_2 (A), (b) W–Mn/SiO_2 (B) and (c) W–Mn/SiO_2 (C) catalysts.

3. Results and discussion

3.1. Catalysts characterization analysis

In order to obtain information about the principle components of these catalysts, X-ray powder diffraction (XRD) was used to identify bulk phases composition and crystal size in different catalysts. The XRD patterns of W–Mn/SiO_2 (A)–(C) are shown in Fig. 1. It can be seen that the main crystallite phases of catalysts were Mn_2O_3, Na_2WO_4 and α-cristobalite. Although the precursors of silica support in these catalysts were different for one another, most of them were transformed into highly crystallite α-cristobalite during calcination except that a little of quartz were detected in W–Mn/SiO_2 (B). Table 1 shows that the crystal size of Mn_2O_3 and Na_2WO_4 in W–Mn/SiO_2 (A)–(C) catalysts were in the range of 61.4–82.1 and 50.7–53.5 nm, respectively.

Table 2 shows the observed binding energy and near-surface elemental concentrations of the fresh catalysts by XPS characterization. As the stoichiometric calculation, the 5 wt% Na_2WO_4–2 wt% Mn/SiO_2 had an average bulk atomic composition of 0.7% Na, 0.35% W, 0.75% Mn and 32.2% Si. By comparison with the bulk compositions, for the W–Mn/SiO_2 (A) catalysts prepared by the incipient wetness impregnation method, surface atomic concentration of Na, W and Mn were 10.0%, 0.5% and 4.6%, respectively, which indicated that Na, W and Mn were enriched on catalyst surface. For the W–Mn/SiO_2 (B) sample, the surface atomic concentration of W and Mn were nearly identical with the bulk composition, while for W–Mn/SiO_2 (C) sample, the W and Mn somewhat migrated to the catalyst surface. On the other hand, it could be seen that the binding energy of Na(1s), W(4f), Mn(2p), Si(2p) and O(1s) did not change with the different catalyst preparations. The oxygen species with O(1s) binding energy of 532.0 was assigned to surface SiO_2, and the oxygen species with O(1s) binding energy of 530.0 was assigned to surface MO_x.

The O_2-TPD profiles of fresh catalysts are shown in Fig. 2. For W–Mn/SiO_2 (A), W–Mn/SiO_2 (B) and W–Mn/SiO_2 (C), there was only one O_2 desorption peak centered, respectively, at ca 935, 920, and 945 °C; the corresponding amounts were 37.6, 30.6, and 59.0 μmol g^{-1}. Many of references [1,3,4,15–17]

Table 1
Phase identification and crystal size of the 5 wt% Na_2WO_4–2 wt% Mn/SiO_2 catalysts

Catalysts	Crystal phase	Size (nm)[a]	Crystal phase	Size (nm)[a]
W–Mn/SiO_2 (A)	Na_2WO_4	50.7	Mn_2O_3	61.4
W–Mn/SiO_2 (B)	Na_2WO_4	52.3	Mn_2O_3	56.8
W–Mn/SiO_2 (C)	Na_2WO_4	53.5	Mn_2O_3	82.1

[a] Particle size was estimated using the Scherrer formula.

Table 2
XPS binding energies (eV) and near-surface compositions (at.%) of the 5 wt% Na_2WO_4–2 wt% Mn/SiO_2 catalyst components

Catalysts	Na(1s)		W(4f)		Mn(2p)		Si(2p)		O(1s) (SiO_2)		O(1s) (MO_x)[a]	
	BE (eV)	at.%	BE (eV)	at.%	BE (eV)	at.%	BE (eV)	at.%	BE (eV)	at.%	BE (eV)	at.%
W–Mn/SiO_2 (A)	1072.4	10.0	35.8	0.5	641.9	4.1	103.4	18.4	532.7	55.4	530.1	11.6
W–Mn/SiO_2 (B)	1072.0	6.3	35.5	0.3	642.1	0.6	103.4	21.5	532.7	65.6	530.2	5.6
W–Mn/SiO_2 (C)	1071.8	6.7	35.5	0.5	641.9	1.0	103.4	21.7	532.6	64.0	530.1	6.0

[a] MnO_x represents the metal oxides except SiO_2.

Table 3
Catalytic performance of 5 wt% Na_2WO_4–2 wt% Mn/SiO_2 catalysts[a]

Catalysts	Conversion (%)		Selectivity (%)				Yield (%)	
	CH_4	O_2	C_2	C_2H_4	CO_2	CO	C_2	C_2H_4
W–Mn/SiO_2 (A)	30.31	96.3	68.36	42.03	21.42	10.21	20.72	12.74
W–Mn/SiO_2 (B)	27.96	97.1	69.34	40.92	17.70	12.96	19.39	11.44
W–Mn/SiO_2 (C)	22.39	65.6	69.36	36.27	23.83	6.82	15.53	8.12

[a] Reaction condition: $T = 820\,^{\circ}C$; $CH_4/O_2 = 4$; GHSV = 30000 ml g^{-1} h^{-1}; 0.2 g catalyst.

reported that the active oxygen species of Na–W–Mn/SiO_2 catalysts were surface lattice oxygen, which desorption began at ca 620 °C and mass-produced at ca 820 °C. In Fig. 5, one can observed that desorption of O_2 began at ca 600 °C for three of W–Mn/SiO_2 samples. Before 800 °C no desorption peak was observed for all samples, indicating no physical and chemical adsorptions of O_2 on W–Mn/SiO_2 catalysts. Because there was one only O_2 desorption peak for each of three samples at higher than 900 °C, the desorbed oxygen should include not only surface lattice oxygen, but also bulk lattice oxygen.

3.2. Oxidative coupling of methane

The results of reactant conversions and product selectivities of 5 wt% Na_2WO_4–2 wt% Mn/SiO_2 catalysts prepared by different methods for OCM are listed in Table 3. The C_2 selectivities of W–Mn/SiO_2 (A), W–Mn/SiO_2 (B) and W–Mn/SiO_2 (C) were comparable under the same reaction conditions, while CH_4 conversion and O_2 conversion of W–Mn/SiO_2 (C) catalyst were evident lower than those of other two catalysts. In addition, over the W–Mn/SiO_2 (C) catalyst, a higher CO_2 selectivity and lower C_2H_4 and CO selectivities were observed.

Fig. 3 shows the influence of temperature for OCM reaction over the W–Mn/SiO_2 catalysts. It should be noted that, the OCM reaction, and more so far the deep oxidation reactions, is very exothermic. The reactor temperature will increase with the accumulation of reaction heat and hot spots will be present in the catalyst bed [11,18–20]. In the present experiments, the increase of temperature in catalyst bed was indeed observed at the beginning of the reaction, but after steady state was reached the temperature of catalyst was 20 °C higher in average than the operation temperature. To be consistent with our previous reports, all the temperature present here referred to the operation temperature. With the increase of temperature from 800 to 820 °C, the conversion of methane and oxygen simultaneously dramatically increased over W–Mn/SiO_2 (A) and W–Mn/SiO_2 (B) catalysts. For W–Mn/SiO_2 (C) catalyst, CH_4 and O_2 conversion increased constantly with the temperature increasing in the range of 780–860 °C, and no leaping increase of those like other two catalysts was observed. The best selectivity of C_2 was occurred at 800 °C for both W–Mn/SiO_2 (A) and W–Mn/SiO_2 (B) catalysts, and at 820 °C for W–Mn/SiO_2 (C) catalyst. It was expected, when oxygen consumption was close to 100%, that there would be a drop in deep oxidation and an increase in C_2 selectivity. However, for Na_2WO_4–Mn/SiO_2 catalysts, a decrease of C_2 selectivity was observed with the temperature increase at the nearly 100% oxygen conversion condition. It suggested that the self of gas oxygen did not participate directly in OCM reaction over Na_2WO_4–Mn/SiO_2 catalysts.

Our previous studies [10,17] have been clarified that the active oxygen species was surface lattice oxygen O_s^{2-} for Na_2WO_4–Mn/SiO_2 catalyst, and transport of gas-phase oxygen molecules to lattice oxygen ions over surface catalytic sites is the key step toward the formation of active oxygen species. Compared catalytic performances with the results of O_2-TPD, W–Mn/SiO_2 (C) catalyst was modest in the capability to activate gas oxygen, which in turn debased the conversion of methane. Because of more desorbed oxygen, W–Mn/SiO_2 (C) catalyst

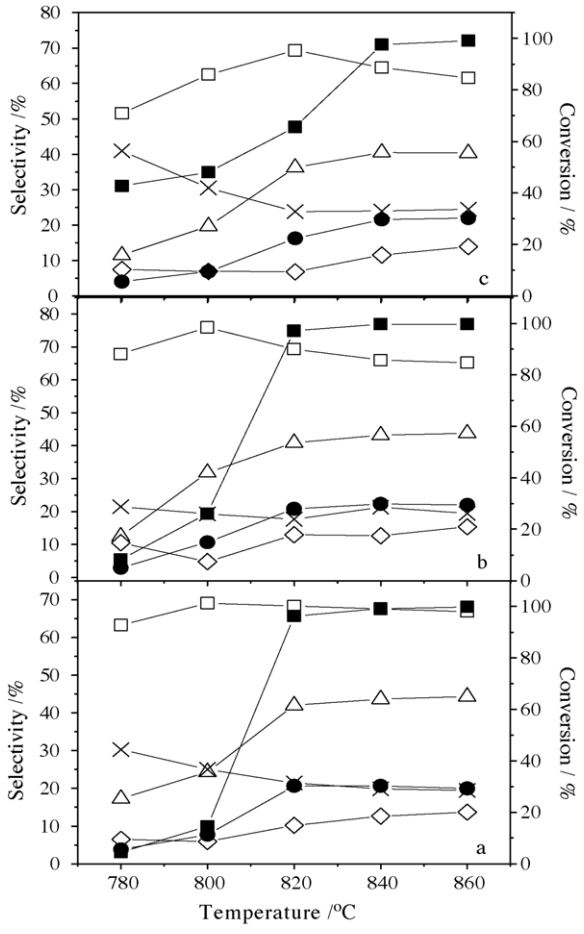

Fig. 3. The catalytic performance of 5 wt% Na_2WO_4–2 wt% Mn/SiO_2 catalysts as related to operation temperatures at GHSV of 30000 ml g^{-1} h^{-1} and CH_4/O_2 of 4. (a) W–Mn/SiO_2 (A), (b) W–Mn/SiO_2 (B), (c) W–Mn/SiO_2 (C). Conversion: (●) CH_4, (■) O_2; selectivity: (□) C_2, (△) C_2H_4, (×) CO_2, (◊) CO.

was not so good as an oxygen-catcher. With the increase of temperatures from 820 °C or 840 °C, C_2 selectivities decreasing and CO selectivities increasing due to the bulk lattice oxygen more likely began to release, which facilitated the deep oxidation process of hydrocarbon. These observations were in agreement with the report in reference [2] that CO was mainly produced by the deep oxidation of C_2 hydrocarbon in OCM reaction.

3.3. Catalyst stability

Based on the data of catalytic performance, one can observe that there were comparable catalytic activities for OCM reaction over 5 wt% Na_2WO_4–2 wt% Mn/SiO_2 catalysts prepared by the incipient wetness impregnation method and mixture slurry method. In addition, the results of XPS indicated, for the catalysts prepared by mixture slurry method and sol–gel method, that the elemental concentrations on surface and in bulk of catalysts were relatively uniform, which was expected to alleviate the loss of active components in long-term reaction. Considering the stability test of Na_2WO_4–Mn/SiO_2 catalysts prepared by the incipient wetness impregnation method have been carried out in our previous works [17,21], only the stability of 5 wt% Na_2WO_4–2 wt% Mn/SiO_2 catalysts prepared by mixture slurry method was investigated in this study.

Fig. 4 shows that W–Mn/SiO_2 (B) catalyst was stable throughout a 500 h run at 800 °C, 3.0×10^4 ml g^{-1} h^{-1} GHSV and $CH_4/O_2 = 2$. CH_4 conversion maintained at 27–31%, C_2 selectivity was 68–71% and C_2H_4 selectivity was 40–46%. With the time on stream, CO selectivity increased from 10% to 20% and CO_2 selectivity decreased from 20% to 10% approximately.

Structure changes in the catalyst used for 500 h reaction were characterized using XRD and XPS methods. In Fig. 5 the XRD patterns show that the crystal state of support SiO_2 changed from α-cristobalite into α-tridymite and SiO_2 quartz; Na, W and Mn could still be detected as the crystallite phases of Na_2WO_4 and Mn_2O_3. Literatures [5,12] reported that the phase transition from amorphous silica to α-cristobalite was a crucially important requirement to generated active and highly selective catalysts, especially with respect to formation of ethylene. However, in our study, the change from α-cristobalite into α-tridymite and

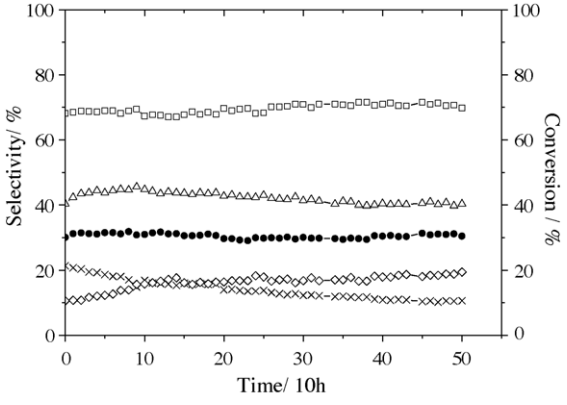

Fig. 4. 500 h stability test over W–Mn/SiO_2 (B) catalyst at GHSV of 30000 ml g^{-1} h^{-1} and CH_4/O_2 of 4. Conversion: (●) CH_4; selectivity: (□) C_2, (△) C_2H_4, (×) CO_2, (◊) CO.

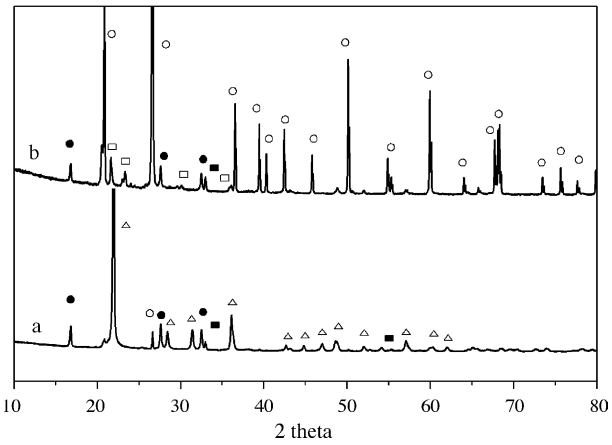

Fig. 5. The XRD patterns of fresh and after 500 h run W–Mn/SiO_2 (B) catalyst: (a) fresh catalyst; (b) 500 h used catalyst. (●) Na_2WO_4, (□) Mn_2O_3, (△) α-cristobalite, (◯) quartz, (□) α-tridymite.

SiO_2 quartz did not significantly influence the activity and selectivity of catalyst. This result suggested that the α-cristobalite in Na_2WO_4–Mn/SiO_2 catalyst can provided high activity and selectivity, but it is not always indispensable.

The surface areas of the fresh and used catalysts are given in Table 4, from which it is evident that reaction after 500 h decreased the surface areas from 3.0 to 1.2 m^2 g^{-1}. This attributed to the phase transition of α-cristobalite. XPS results obtained on the fresh W–Mn/SiO_2 (B) catalyst and after 500 h on stream are shown in Table 4. There was an increase in Na, W and Mn concentrations on catalyst surface after an extended time on stream. The fact that these elements concentrations increased with the time on stream was consistent with the sustained activity and selectivity of this catalyst. However, studies on the 450 h catalyst prepared by he incipient wetness impregnation method revealed that 97% of the tungsten species observed on the fresh catalyst by XPS disappeared [17]. In comparison with the catalyst prepared by the incipient wetness impregnation method, it was the uniform elemental concentrations between surface and bulk of W–Mn/SiO_2 (B) catalyst that made elements migrate from bulk to surface and counteracted the loss of active components during the reaction. What the elements migrated from bulk to surface could be explained as follows: firstly, with time on stream, under OCM reaction conditions, Na, W and Mn doped in the bulk of W–Mn/SiO_2 (B) catalyst inclined to move towards the surface of catalyst accompanying with the crystal perfection of SiO_2; secondly, the relatively poor oxygen atmosphere induced the metals to shift from the bulk to the surface of catalyst.

Table 4
Near-surface compositions (at.%) of W–Mn/SiO_2 (B) catalyst components and surface areas

Catalyst	Na(1s)	W(4f)	Mn(2p)	Si(2p)	O(1s)		Surface area (m^2 g^{-1})
					SiO_2	MO_x[a]	
Fresh	6.3	0.3	0.6	21.5	65.6	5.6	3.0
Used	6.4	0.8	0.9	23.2	63.5	5.0	1.2

[a] MnO_x represents the metal oxides except SiO_2.

Hence, the Na_2WO_4–Mn/SiO_2 catalyst prepared by the mixture slurry method exhibited excellent stability.

4. Conclusion

The incipient wetness impregnation method was most extensively applied to prepare W–Mn/SiO_2 catalysts as tradition, and provided excellent catalytic activity for OCM reaction. By controlling the preparation conditions, the 5 wt% Na_2WO_4–2 wt% Mn/SiO_2 catalysts prepared by the mixture slurry method could obtain similar activity comparing with the incipient wetness impregnation method. The catalyst prepared by sol–gel method exhibited a modest capability to activate oxygen and methane. For all samples prepared by different methods, the main crystallite phases were Mn_2O_3, Na_2WO_4 and α-cristobalite, and the different precursors of silica were transformed ultimately into highly crystallite α-cristobalite. For the catalyst prepared by incipient wetness impregnation method, Na, W and Mn were mainly distributed on the surface of catalyst. While those catalysts prepared by latter methods, the elements distribution were more uniform between the surface and bulk. 500 h stability test showed that the mixture slurry method could alleviate the loss of active components and provided an excellent stability. Although the α-cristobalite was considered as an important requirement for the production of effective catalyst, the structure change of support SiO_2 after 500 h run indicated that it was not always indispensable for high active and selective.

Acknowledgments

Financial supports from the Ministry of Science and Technology of China (Grant 1999022406) and Nature Science Foundation of China (Grant 20378081) are gratefully acknowledged.

References

[1] X. Fang, S. Li, J. Gu, D. Yang, J. Mol. Catal. (China) 6 (1992) 255.
[2] X. Fang, S. Li, J. Lin, Y. Chu, J. Mol. Catal. (China) 6 (1992) 427.
[3] Z. Jiang, C. Yu, X. Fang, S. Li, H. Wang, J. Phys. Chem. 97 (1993) 12870.
[4] D. Wang, M.P. Rosynek, J.H. Lunsford, J. Catal. 155 (1995) 390.
[5] A. Palermo, J.P.H. Vazquez, A.F. Lee, M.S. Tikhov, R.M. Lambert, J. Catal. 177 (1998) 259.
[6] Y. Liu, Ph.D. Dissertation, Lanzhou Institute of Chemical Physics, Chinese Academy of Sciences, 1997.
[7] L. Chou, Y. Cai, B. Zhang, J. Niu, S. Ji, S. Li, Chem. Commun. (2002) 996.
[8] L. Chou, Y. Cai, B. Zhang, J. Niu, S. Ji, S. Li, Appl. Catal. A 6180 (2002) 1.
[9] L. Chou, Y. Cai, B. Zhang, J. Niu, S. Ji, S. Li, React. Kinet. Catal. Lett. 76 (2002) 311.
[10] S. Li, Chin. J. Chem. 19 (1) (2001) 16.
[11] S. Pak, J.H. Lunsford, Appl. Catal. A168 (1998) 131.
[12] A. Palermo, J.P.H. Vazquez, R.M. Lambert, Catal. Lett. 68 (2000) 191.
[13] S. Ji, T. Xiao, S. Li, C. Xu, R. Hou, K.S. Coleman, M.L.H. Green, Appl. Catal. A 225 (2002) 271.
[14] S. Ji, T. Xiao, S. Li, L. Chou, B. Zhang, C. Xu, R. Hou, A.P.E. York, M.L.H. Green, J. Catal. 220 (2003) 47.
[15] J. Wu, S. Li, J. Niu, X. Fang, Appl. Catal. A 124 (1995) 9.
[16] J. Wu, S. Li, J. Phys. Chem. 99 (1995) 4566.
[17] Y. Kou, B. Zhang, J. Niu, S. Li, H. Wang, T. Tanaka, S. Yoshida, J. Catal. 173 (1998) 399.
[18] A. Kooh, J.L. Dubois, H. Mimoun, C.J. Cameron, Catal. Today 6 (1990) 453.
[19] D. Schweer, L. Mleczko, M. Baerns, Catal. Today 21 (1994) 357.
[20] A. Malekzadeh, M. Abedini, A.A. Khodadadi, M. Amini, H.K. Mishra, A.K. Dalai, Catal. Lett. 84 (2002) 45.
[21] J. Lin, J. Gu, D. Yang, C. Zhang, Y. Yang, Y. Chu, S. Li, Pertrochem. Technol. (China) 24 (1995) 293.